Project Title:

Prediction of Crystal Structure and Properties

Name: ○Toshiaki Iitaka, Yanming Ma, John Sak Tse, Zhi Li

Laboratory at RIKEN: Computational Astrophysics Lab

1. Background and purpose of the project, relationship of the project with other projects

The recent discovery of the phase IV of hydrogen—a mixed structure composed of layers of molecular units as well as weakly bonded graphene-like sheets—has generated much excitement. However, solid hydrogen remains insulating at pressure up to at least 320 GPa, and thus its potential superconductivity is still beyond realization. Another way toward the metallization of hydrogen and concomitant superconductivity may be via doping, for example, by an electropositive alkali or alkaline earth element.

Computational studies of the alkali/alkali-earth metal polyhydrides, MH_n with n >1/n>2, show that these species become stable with respect to decomposition into MH/MH_2 and H_2 at pressures ranging from 2 GPa for cesium[5] to 100 GPa for lithium[3] and that lower ionization potentials lead to lower stabilization pressures. The structures they adopt differ greatly, especially in their hydrogenic sublattices. Our predicted calcified species are particularly interesting because the most stable stoichiometry above 150 GPa, CaH_6, has a body-centered cubic structure with hydrogen that forms unusual "sodalite" cages containing enclathrated Ca. The stability of this structure is derived from the acceptance by two H_2 of electrons donated by Ca forming an "H_4" unit as the building block in the construction of the three-dimensional sodalite cage. This unique structure has a partial occupation of the degenerated orbitals at the zone center. The resultant dynamic Jahn–Teller effect helps to enhance electron– phonon coupling and leads to superconductivity of CaH_6. A superconducting critical temperature (Tc) of 220–235 K at 150 GPa obtained from the solution of the Eliashberg equations is the highest among all hydrides studied thus far.

The current research project initially aims to explore the high pressure crystal structures on hydrogen rich hydrides of MH_n, (M=Ni, Cu and Zn, n ⩾ 2) through our CALYPSO (Crystal structure AnaLYsis by Particle Swarm Optimization) method on crystal structure prediction, thus zero temperature high pressure phase diagram can be established. I then wish to perform extensive electron-phonon coupling calculations using the predicted high pressure metallic structures within the linear response theory to understand if these compounds can be superconducting at high pressures. However, after a great effort on this system I have only found several interstitial alloys, e.g. CuH, NiH, but polyhydrides, MH_n with n ⩾ 2, is energetically unstable at high pressures upto 400 GPa. It is well known that those interstitial alloys are good conductors but not high temperature superconductor. Considering that pressures above 400 GPa is beyond the capability of current DAC technique for polyhydrides, I turn to H_nM, (M=Cl, Br and I; n⩾2) and a deep investigation of BeH_n and SrH_n with n⩾2 in time.

The ultimate goal of the current research is then targeting to reveal the possibility of high temperature superconductivity on these hydrides under ultra-high pressure and to understand the exciting chemistry of hydrogen and the role played on the superconductivity, guiding the future experimental exploration on high temperature superconductivity at high pressures. We expect the current research project could establish important underlying physics on the superconductivity of

hydrogen-rich compounds and also lead us high standard publications in top journals, such as Physical Review Letters or PNAS.

2. Specific usage status of the system and calculation method

During the fiscal year 2013, I have used all of the total allocated CPU time of CPU hours for above calculations.

Ab initio crystal structure prediction has been performed through our newly developed particle swarm optimization technique, which has been implemented in our CALYPSO code. This method is able to search for the structure possessing the lowest free energy at given Pressure-Temperature conditions and is capable of predicting the stable structure of a given compound for a given composition. The structural relaxations were performed with the VASP code. We use plane wave basis sets for the expansion of the electronic wave function, a pseudopotential description of the electron-ion interactions and density function theory (DFT) for the electron-electron interactions through Quantum-ESPRESSO packages. It can calculate the ground-state energy and Kohn-Sham orbitals for both insulators and metal, in any crystal structure, for different exchange-correlation functions. The calculation of the phonon dispersion curves is performed within the direct supercell method via Phonopy package or the linear response theory based on the DFT via Quantum-ESPRESSO.

3. Results

We have explored the structures of BeH_n (n = 1 – 12) and H_nCl (n = 1 – 7) hydrides. For each stoichiometry, calculations were performed at pressures 100-300 GPa with up to four formula units in the model. The enthalpies of candidate structures relative to the products of dissociation into BeH_2/HCl + solid H_2 at the appropriate pressures are calculated. With structure optimization of all the candidate structures, we draw a conclusion which can be seen in Fig.1 that: BeH_2 would be the only stable hydride in the whole pressure range where all the other hydrogen rich compounds tend to dissociate. Therefore, mixing hydrogen with BeH_2 under pressure does not appear to be a promising route toward metallizing hydrogen

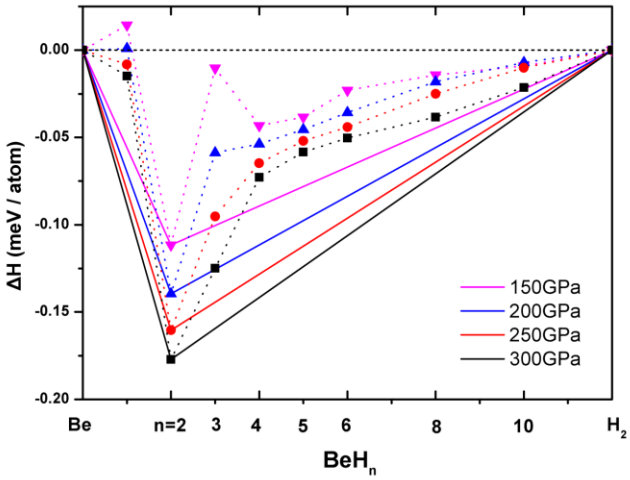

Fig. 1 | Enthalpies of formation (ΔH, with respect to Be and H_2) of BeH_n (n = 1 – 12) and crystal structures. The abscissa x is the fraction of H_2 in the structures.

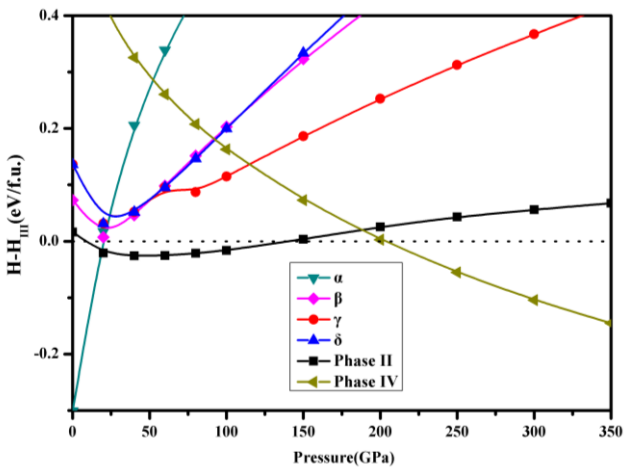

Fig. 2 | Calculated enthalpies (relative to phase III) of various structures as function of pressure in BeH_2.

The dynamical stable BeH_2 compound has went through a series of phase transition. Results of the structure searches are summarized in Fig. 1 where the enthalpies of the most energetically competitive structures of BeH_2 for the pressure range 0-350 GPa are presented.

The ambient stable phase *α* observed by experiments transits to the 1T structure (denoted as phase II) at around 20 GPa, and it remains so up to 141 GPa. Above 141 GPa the *R*-3*m* structure (phase III) takes

over the stability and it further transforms to the *Cmcm* structure (phase IV) at 202 GPa.

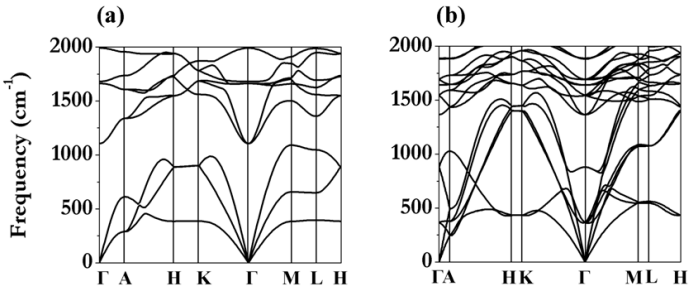

Fig. 3| Calculated phonon dispersion curves of BeH_2 with P-3m1 structure at 100 GPa (a), R-3m structure at 150 GPa (b), respectively.

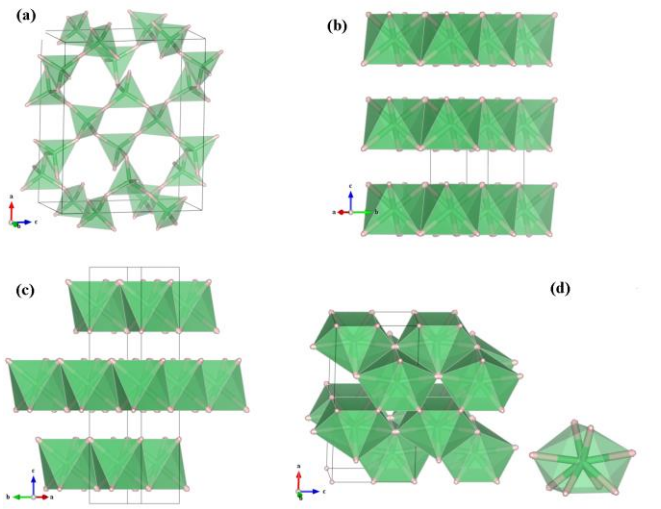

Fig. 4| Crystal structure of BeH_2 (a) The experimental α-BeH_2. (b) The P-3m1 structure (phase II) (c) The R-3m structure (phase III). (d) The *Cmcm* structure (phase IV). The BeH_8 hendecahedral unit which builds the Be-H network in phase IV is specified in Fig.1(d)

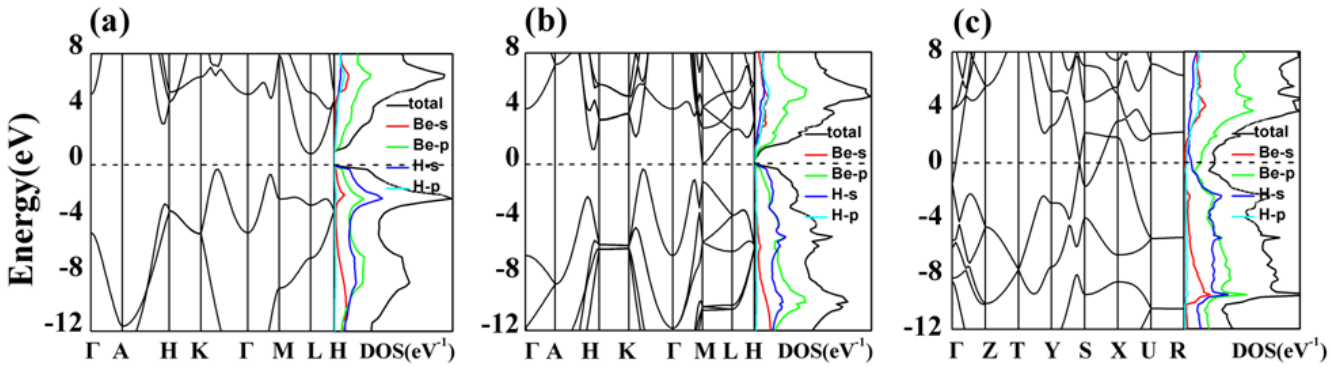

Fig. 5| Calculated band structure, partial and total electronic DOS (right panel) for P-3m1 structure at 100 GPa (a), R-3m structure at 200 GPa (b), and Cmcm structure at 210 GPa (c), respectively

To investigate the zero-point motion effects on phase stability, we have estimated the ZPEs at 100-250 GPa within quasi-harmonic approximation as listed in Table II. Though the absolute ZPEs are reasonably large, the differences of which are quit small at a certain pressure. As a result, the inclusion of ZPEs in the phase diagram shifts slightly the transformation pressures into phase III and IV, while the phase transition sequence remains unaltered. In the phonon calculations, the stability of three phases has also been confirmed by the absence of imaginary phonon frequency in the whole Brillouin zones, as shown in the calculated phonon spectrum (Figs.3 and 6).

The structure of the crystalline *α* phase is presented in Fig. 4a. This structure is composed of body-centered orthorhombic unit cells with a network of corner-sharing BeH_4 tetrahedra. Unlike heavier alkaline-earth metals, beryllium is bonded with hydrogen by mainly covalent bonds, rather than ionic ones, due to its small atomic size and high ionization energy. Upon increasing pressure, the *α* phase would transform to the 1T structure (Fig. 4b). The 1T structure consists of hexagonal close-packed BeH_2 slabs formed by edge-sharing BeH_6 octahedra. Within each slab, half of the octahedral voids are

filled by Be atoms. Each Be atom is surrounded by six H atoms in an octahedral arrangement, while each H atom is connected to three Be atoms. At 50 GPa, the average intra-layer Be-H bonding length is 1.42 Å and inter-layer H…H distance is 1.64 Å. The slabs of BeH_2 consist of covalent Be-H bonds, which is not so different from the bonding of the *α* phase. The electron octet is already fulfilled within individual slabs, and therefore the bonding across the slabs is very weak, essentially by van der Waals forces. Near 141 GPa, the 1T structure will transform to a rhombohedral *R*-3*m* structure. The *R*-3*m* structure and the 1T structure are both built up from the BeH_2 layers of same geometry and only differ in their stacking sequence (Fig. 4c). All BeH_2 layers are equivalent in the 1T structure thus there is only one BeH_2 layer per unit cell. The *R*-3*m* structures on the other hand have three non-equivalent BeH_2 layers, forming a ABCA stacking in the unit cell. There are more than two choices of stacking sequences. We have examined all possible varieties and found that no other stacking patterns are energetically more competitive than the 1T or *R*-3*m* structures. At sufficient compression the dihydrogen bonding would be strong enough to destabilize the layer structures and induces another phase transition. We predicted that the *R*-3*m* structure would become unstable near 200 GPa and transform to the *Cmcm* structure (Fig. 4d). The *Cmcm* structure has a three-dimensional extended Be-H network consisting of eight-coordinated BeH_8 hendecahedrons. This topology of atomic configuration is fully different from the layered phase II and III. The average Be-H bonding length of phase IV is nearly unchanged from phase III however, the electrons are more delocalized in phase IV which gives rise to the metallization.

The electronic properties of the three phases of BeH_2 were systematically investigated by density of state (DOS), band structure and Bader charge analysis calculations. The predicted phases II and III are insulating phases with sizable energy gaps (Figs. 5a and 5b). In both structures, the magnitude of the band gaps decease with increasing pressures as the molar volume decreases – when the van der Waals gap reduces, the orbital overlaps across the gap is enhanced. However the band gap closure will not eventually appear in phase III, because of the layered structure. Instead, the phase III would transform to a denser packing of the atoms, to wit the phase IV, and reaches the metallic state concurrently. As shown in Fig 4c, the calculated band structure and DOS reveals that phase IV is indeed metallic with Be-*p* and H-*s* orbitals dominate the density of states at the Fermi level. The density functional calculation is known to underestimate the band gap, so we performed the calculations using a hybrid functional where 25% of the GGA exchange potential is replaced by screened Fock exchange. This type of Heyd–Scuseria–Ernzerhof (HSE) hybrid functional can revises the underestimate and thus usually provides a better description of the electronic band structure. The calculation shows that a band closure still exists in phase IV which is consistent with the conclusion derived from PBE calculation. Our results therefore suggest that the metallization of BeH_2 should be achieved at 202 GPa through a reconstructive III → IV transition featuring a dramatically topological change of atom configurations.

Metallic high-pressure phases of hydrogen-rich compounds hold a promise as high-temperature superconductors. To explore the superconducting properties, we calculated the electron-phonon coupling (EPC) parameter, λ, the logarithmic average phonon frequency, ωlog, and the electronic DOS at the Fermi level, $N(E_f)$, for the phase IV, at 250 and 300 GPa. According to our calculations, at 250 GPa, λ reaches 0.63, and ωlog is 1729 K, so that the estimated Tc within Allen-Dynes modified McMillan equation becomes ~38 K, considering typical Coulomb pseudopotential parameters, μ*, of 0.12.

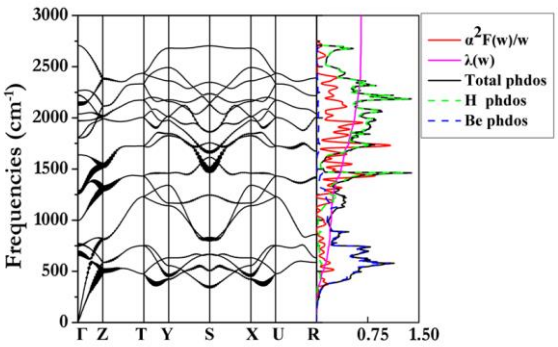

Fig. 6 | (Left) Calculated phonon band structure for Cmcm BeH2 at 300 GPa. Solid circles show the electron-phonon coupling with the radius proportional to their respective strength. (Right) The Eliashberg phonon spectral function, α2F(ω), and the partial electron-phonon integral, λ(ω) , are compared to the phonon DOS projected on Be and H atoms.

With increasing pressure, the calculated λ and the resulting Tc increase up to 41 K at 300 GPa. The large Tc of the phase IV is mainly attributed to the strong electron phonon coupling, λ, and the high ωlog. In order to understand the origin of this strong λ, we also calculated the Eliashberg phonon spectral function, α2F(ω)/ω, and the partial electron-phonon integral, λ(ω), as shown in Fig. 6. Note that the low-frequency vibrations which are mainly associated with Be atoms due to their relatively higher atomic mass, provide a contribution of 30% of the total EPC parameter, while the phonon frequencies between 1300–1700 cm-1 account for nearly 50% of λ. To further explore the contribution associated with different phonon modes, solid circles with the radius proportional to the electron-phonon coupling are also plotted in Fig. 6. The calculated phonon linewidths showed that the electron–phonon coupling is mostly derived from S point. Phonon modes between 1300 and 1600 cm-1 along Y-S-X are primarily responsible for the main peak in the Eliashberg phonon spectral function, α2F(ω)/ω, and yield an important contribution to λ. Furthermore, these phonon modes are predominated by the vibration of H atoms. We therefore conclude that the high-pressure superconductivity is more related to the high-energy H modes than low-energy Be modes.

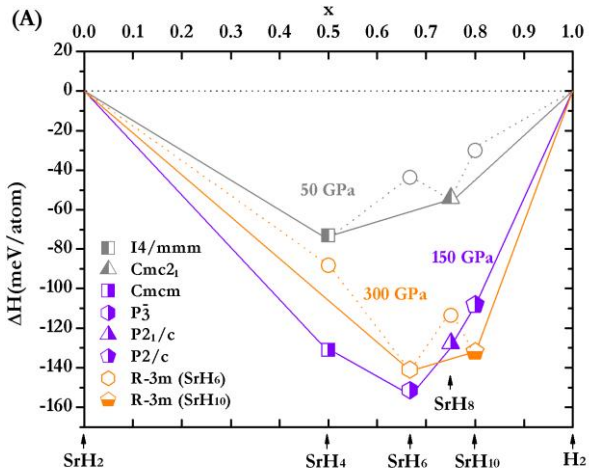

Fig. 7 | Enthalpies of formation (ΔH, with respect to Sr and H_2) of SrH_n (n = 2 – 10)

The lowest-enthalpy structures, stable relative to SrH_2 and H_2, at different SrH_x stoichiometries and pressures are depicted in the convex hull plot (Fig. 7). A structural feature common to all SrH_x below 100 GPa is the existence of molecular H_2 and atomic H^-. At higher pressures, while the crystal structures of SrH_4 and SrH_8 retain these two H species, SrH_6 and SrH_{10} exhibit a wide bonding diversity. The most intriguing structural modification was seen in SrH_6. The low pressure *C*2/*c* structure was found to transform at 75 GPa to a R-3m structure. Both structures are formed from H_2 and H^- units. At 200 - 250 GPa, bent H_3^- species was found in the *P*321 structure. Above 250 GPa, the bent H_3^- units are linked to form a spiral polymer chain running along the c axis of the new R-3m structure. Furthermore, the hydrogen in SrH_{10} evolved from H_2 and H^- in the $P2_1/m$ structure at 50 GPa, to H_2 and bent H_3^- species in the *P*2/*c* structure at 150 GPa, and eventually to H^- and novel distorted H_4 tetrahedra units in the R-3m structure at 300 GPa. In comparison, over the pressure range (< 300 GPa), the SrH_2 polymorphs show only hydridic H^- species.

Electronegativity is a chemical property that describes the tendency of an atom or a functional

group to attract electrons. The Mulliken scale defines electronegativity χ as the arithmetic mean of the ionization potential and the electron affinity. From density functional theory, the Mulliken electronegativity of molecular H_2 was calculated to be 5.441 eV. The Mulliken scale can be converted to the more common Pauling scale using a recent formula[21] which yields χ(Pauling) = 1.71 for a H_2 molecule. It is important to note that the estimated Pauling electronegativity of molecular H_2 is close to the group 13 and 14 elements (1.61–2.33). Considering the electronegativity of Sr (χ(Pauling) = 0.95), the large electronegativity difference ($\Delta\chi$ = 0.76) between Sr and H_2 is the primary reason for the ionic solid structure in SrH_2. This observation is significant because Zintl-phase compounds are known composed of electropositive metals (e.g., alkali, alkaline earth, and rare earth metals), and electronegative metals around the "Zintl line", which divides group 13 and 14 in the periodic table. The similarity of the electronegativity of H_2 with those of the group 13 and 14 elements suggests that the Zintl-Klemm principle is applicable to describe the structures of high pressure SrH_x polymorphs. Thus, it is plausible to explain the various H species formed in crystalline SrH_x by assuming that the H_2 molecule(s) has (have) accepted the two valence electrons donated by the Sr atom and by the consideration of the Coulombic interactions between the charged ions.

Examination of the structures of the high pressure polymorphs in SrH_x and group 1 and 2 polyhydrides suggests structures of the H^-containing units are determined by the competition of the energies of the products resulting from the Sr → H_2 charge transfer as the combinations of H^-, H_2, H_2^-, and H_3^- species. For this purpose, accurate coupled-cluster calculations with single, double and triplet excitations (CCSD(T)) were performed by using an almost complete aug-cc-pV6Z basis set for the relevant H-species (Table 1). It should be emphasized that highly correlated calculations are essential to provide accurate total energies for small hydrogen clusters. Density functional calculations with the current functionals fail due to the neglect of self-interaction corrections. The resultant CCSD(T) total energies of the relevant H species are listed in Table 1. The data allow calculations of the relative energies of possible combinations of the H fragments present in the SrH_x structures.

Table 1. Total energies (ET, (a.u.)) for various H species predicted in the high pressure structures of SrH_x, and the calculated total energies per H_2 for various combinations of the H fragments.

Species	**r(H-H) / Å**	**ET**
H		-0.4999993
H^-		-0.5275453
H_2	0.7416	-1.1743599
H_2^-	0.7452	-1.1378338
H_3^-	1.0585	-1.6848445

	Reactions	ET/H_2
SrH_4	$2H_2 + 2e \rightarrow 2H_2^-$	-1.1378
	$\rightarrow H^- + H_3^-$	-1.1049
	$\rightarrow 2H^- + H_2$	-1.1647
SrH_6	$3H_2 + 2e \rightarrow 2H_3^-$	-1.1215
	$\rightarrow H_3^- + H^- + H_2$	-1.1281
	$\rightarrow$ **$2H^- + 2H_2$**	-1.1346
SrH_8	$4H_2 + 2e \rightarrow 2H_3^- + H_2$	-1.1347
	$\rightarrow H_3^- + H^- + 2H_2$	-1.1396
	$\rightarrow$ **$2H^- + 3H_2$**	-1.1445
SrH_{10}	$5H_2 + 2e \rightarrow 2H_3^- + 2H_2$	-1.1426
	$\rightarrow H_3^- + H^- + 3H_2$	-1.1466
	$\rightarrow$ **$2H^- + 4H_2$**	-1.1505

The calculated energetics show the combination of H^- and H_2 has the lowest energy, and therefore should be the preferred structural units in SrH_x. Indeed, the predicted structures of SrH_x show the bonding patterns of hydridic H^- anion + molecular H_2 up to 100 GPa. Note that over this

pressure range the H_2 bond lengths among the SrH_x polymorphs fall in between 0.77 - 0.79 Å, which is comparable to that of the isolated H_2 molecule. The shortest Sr^{2+}… H^- contacts in SrH_x are all within 1.87–1.93 Å and are not sensitive to the crystal structures. Thus, the Coulombic contribution (Madelung energy) to the total energy should be similar in these structures. Incidentally, the stable structures of CaH_x (x = 4, 6, 8, and 10), MgH_x (2 < x < 6), and $M_{AM}H_x$ (x > 1, M_{AM}= Cs, Rb and K) also share the H_2 + H^- units. This observation supports that the simple charge-transfer energetic model proposed here is also applicable to describe the structural patterns in related systems. Molecular $[H_2]^{\delta-}$ units, however, are observed in high pressure group 1 and 2 polyhydrides with predominant H_2 concentration. This is easily understood from the consideration of the number of "effectively added electrons" donated from the metal to the H_2 σ* bonds. If the additional electrons from Sr are shared among all the H_2 molecules, there are not enough electrons to fully populate σ* bonds and the molecular structure is maintained. This principle is consistent with the predicted lowest enthalpy high pressure structures of hydrogen-rich CaH_{12}, MgH_{12} and MgH_{16}.

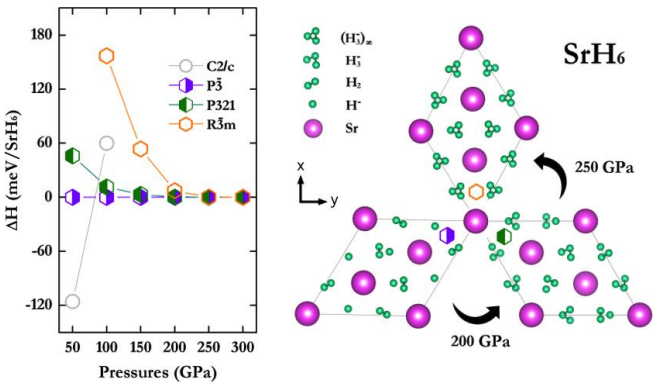

Fig. 8 | Enthalpies and the scheme of phase transition.

Above 100 GPa the successive phase transitions found in SrH_6, manifest the diversity of the chemical bonding in the solid state. As shown in Fig. 8, the calculated enthalpies show the P-3 and *P*321 structures are energetically competitive in the pressure range 150-200 GPa and almost degenerate with the R-3m structure above 250 GPa. At 200 GPa, the H^-…H_2 units in SrH_6 are compressed close to each other and linked to form H_3^-. This is the driving mechanism for the P-3 → *P*321 phase transition.

4. Conclusion

The phase diagram of BeH_{2n} and H_nCl (n = 1 – 6) hydrides at zero temperature were established. Three phases of BeH_2 were predicted to be stable at different pressure ranges. The 1T layered structure that is normally seen in transition metal dichalcogenides is found to be a stable form of BeH_2 at pressures from ~ 20 GPa up to ~130 GPa. The 1T structure has an insulating electronic state. At higher pressure, another insulating structure with the *R*-3m symmetry becomes more stable. The *R*-3*m* structure is composed from identical BeH_2 layers as the 1T structure but differs from the latter in the stacking sequence. Further increasing pressure to above ~200 GPa, the *R*-3*m* phase undergoes a structural transition from an insulating phase to a metallic phase and changes the structural symmetry to *Cmcm*. Moreover, the estimated superconducting critical temperature T_c of BeH_2 reaches 45 K at 300 GPa by application of the Allen-Dynes modified McMillan equation, indicating that the metallic phase of BeH_2 is potentially also a superconducting state, with an operational temperature attainable in laboratory.

The survey of the most stable high pressure polymorphs of Sr polyhydrides—via study of the reaction of Sr with H_2—has revealed the occurrence of a variety of H bonding motifs. The electronegativity of molecular H_2 was found to be similar to those of the group 13 and 14 metals that form Zintl-phase alloys with group 1 and 2 elements. It is remarkable that the evolution of the crystal

structures predicted can be elucidated via a complete transfer of Sr valence electrons to H_2 in view of the certainly oversimplified assumption. The simple Zintl–Klemm principle is shown to provide insights into a logical understanding of the structural complexity of the Sr polyhydrides.

5. Schedule and prospect for the future

I have been a RICC general user and wish to continue using the system. During the fiscal year 2012, I have performed systemically structure predictions on MH_n, (M=Ni, Cu and Zn, n⩾2) at pressures upto 400 GPa. However, after a great effort on this system I have only found several interstitial alloys, e.g. CuH, NiH, but polyhydrides, MH_n with n ⩾ 2, is energetically unstable at high pressures upto 400 GPa. It is well known that those interstitial alloys are good conductors but not high temperature superconductor. Considering that pressures above 400 GPa is beyond the capability of current DAC technique for polyhydrides, I turn to a deep investigation of BeH_2 and SrH_n with n⩾2 in time. I have performed systemically structure predictions on electronic band structures, phonons, electron-phonon calculations on BeH_2 and SrH_n (n = 2–10) hydrides. The investigations have been finished and I got 2 papers submitted to JCP and JACS, respectively.

For the next fiscal year 2014, we plan to continue using RICC supercomputer to perform the calculations on H_nM (M=Cl, Br; n⩾2), then we will extend our research on the crystal structure prediction of other systems, e.g. MH_n (M= Sc and Ti; n⩾2) and SiH_4, through CALYPSO code, and build the zero pressure phase diagram. We expect high standard publications can be eventually achieved.

Fiscal Year 2013 List of Publications Resulting from the Use of RICC

[Publication]

1. Hui Wang, **John S. Tse**, Ziwei Wang, **Toshiaki Iitaka**, and **Yanming Ma**, "Unusual Hydrogen Species in Dense Strontium Hydrides", **J. Am. Chem. Soc. (2014), submitted.**

2. Ziwei Wang, Yansun Yao, Li Zhu, Hanyu Liu, **Toshiaki Iitaka**, Hui Wang and **Yanming Ma**, "Metallization and Superconducting of BeH_2 Under High Pressure", **J. Chem. Phys. (2014), submitted.**

[Proceedings, etc.]

[Oral presentation at an international symposium]

[Others]